Effects of Mechanical Anisotropy on Core Strain Measurements for In-situ Stress Determination

G. G. Ramos and J. J. Rathmell
ARCO Oil and Gas Co., Plano, Texas

ABSTRACT

On-site strain measurements were made on low permeability, low porosity sandstone core samples with the objective of predicting the azimuth of in-situ stresses. The initial on-site strain tests on 2 wells gave 2 orthogonal azimuths. Thus, laboratory strain, sonic velocity, and macro- and micro-fracture mapping were used to resolve apparent inconsistencies in the initial on-site strain tests. The major axes of compressibility anisotropy and velocity anisotropy closely coincide with the strike of visible coring-induced fractures. From these core anisotropy tests, the inferred orientation of the maximum horizontal in-situ stress is in the azimuth range of 75 +/- 45 degrees. Microscopic examination of thin-sections revealed a major set of aligned microfractures and a second but minor set of microfractures orthogonal to the major set. The major set of uninvaded, intergranular microfractures, presumably the result of strain-relief, is perpendicular to the azimuths of maximum compressibility and minimum sonic velocity.

INTRODUCTION

On-site strain relief tests were applied to tight-gas sandstone cores from two vertical wells in Texas, denoted here as Well #1 and #2, with the aim of determining the azimuth of the maximum horizontal in-situ stress. The tight sandstone is very fine- to fine-grained quartzose sandstone, 70%-90% monocrystalline quartz. Porosity and permeability are low, less than 8% mean porosity and less than 0.008 md air permeability. The initial on-site strain tests on Well #1 gave a maximum strain azimuth of 0-30 degrees, but Well #2 indicated an azimuth of 90-120 degrees, a difference of 90 degrees.

In the geographic region around the subject wells, the general direction of the maximum horizontal in-situ stress and hydraulic fractures have been determined by other investigators. For example, in Gas Research Institute's Staged Field Experiments (GRI-SFE), downhole stress tests give a fracturing direction of 76 degrees, a microseismic survey indicates a hydraulic fracture azimuth of 69 degrees, wellbore ellipticity suggests 68 degrees, differential strain analysis predict 90 degrees, and on-site (anelastic) strain tests have maximum strain azimuths of 69-102 degrees (Owen, Toronto, and Petersen, 1988). In other production wells, south of the SFE site, anelastic strain and velocity anisotropy predict hydraulic fracture azimuths of 62-77 degrees (Teufel, 1983). Therefore, data from these investigators suggest that in the vicinity of Well #1 and #2, the far-field or regional

horizontal in-situ stress has a maximum that lies within the azimuth range of 62-102 degrees, supporting the results of Well #2's on-site strain tests.

In view of the lack of agreement between the on-site strain tests of Well #1 and Well #2, other laboratory test methods, namely differential strain and velocity anisotropy were employed. The preferential orientation of the microcracks was then verified using thin-section fluorescence microscopy. Results of the thin-section microfracture study were used to interpret and reconcile the data from all the core tests.

THEORETICAL BACKGROUND

The orientation of in-situ stresses, which controls the direction of hydraulic fractures, can be measured with several direct and indirect techniques (See for example Lacy, 1987). Techniques that rely on core data have the advantage of lower cost when compared to down-hole methods. Indirect core-based methods assume that preferentially oriented microcracks are developed in the core as a result of stress-relief. The principal stresses in a deep reservoir, Figure 1, are:

$$S_v > S_{hmax} > S_{hmin}$$

where S_v = vertical in-situ stress
S_{hmax} = maximum horizontal in-situ stress
S_{hmin} = minimum horizontal in-situ stress

In general, hydraulic fractures are propagated parallel to S_{hmax}. It has been shown that immediately after cores are recovered from deep formations, the cores adjust to the stress-free environment by expanding. Expansion is maximum along the azimuth of S_{hmax}. It is a result of the generation of preferentially oriented microcracks (Teufel, 1981, 1983). A horizontal cross section of a core sample (Figure 1) will contain stress-relief micro-cracks whose preferred orientation is perpendicular to the maximum horizontal stress, S_{hmax}. There would be a smaller number of microcracks perpendicular to the minimum horizontal in-situ stress, S_{hmin}. The orientation of the microcracks is inferred from core anisotropy tests such as on-site anelastic strain tests, laboratory stress-strain tests, and ultrasonic velocity anisotropy tests. Teufel et al (1984) demonstrated the reliability of these core methods by comparing their predictions to the observed direction of hydraulic fractures in mine-back experiments.

ON-SITE ANELASTIC STRAIN RELIEF TESTS

The on-site anelastic strain relief or relaxation method is based on the time-dependent expansion that occurs immediately after recovery of the core. Ideally, the direction of maximum expansion during relaxation, also referred to as anelastic strain, is parallel to the reservoir maximum in-situ stress

(Blanton and Teufel, 1983; Teufel, 1981). Strain measurements (or the amount of expansion per unit length) are performed near the rig as soon as the core is extracted from the core barrel, hence the name "on-site". In 1985, we contracted a service laboratory to develop equipment and methods for relaxation strain tests, leading to the current commercial system, Figure 2, that has been successfully used in other wells (Toronto and Owen, 1988).

In addition to the basic assumptions of homogeneity and isotropy, the critical factors in making reliable on-site strain tests are core "freshness" or relative age of the core sample (i.e. the number of hours that the sample has spent in the core barrel), stable instrumentation, and a good scribe reference. In deep wells however, after cutting 60 ft of core at 2-4 ft/hr and a trip time of 4 hrs, the only useful sample is the rock at bottom of the core barrel. An example of a strain-time plot, Figure 3, shows core expansion that diminishes with time.

There are 1100 ft of core and 17 tests in Well #1, while there are 240 ft of core and 6 tests in Well #2. The azimuths of the maximum relaxation strains are plotted in rosette diagrams such as Figure 4, using true North as reference. In Well #1, Figure 4A, the azimuth range containing the highest frequency is the 0-30 degree sector. In Well #2, Figure 4B, the dominant sector is 90-120 degrees. Thus, these two wells, merely five miles apart, give different predictions on the azimuth of the regional in-situ stresses, Well #1 shows an azimuth of 0-30 degrees, while Well #2's prediction is 90-120 degrees, perpendicular to that of Well #1. Since these on-site data are inconclusive, laboratory core anisotropy tests were performed.

LABORATORY DIFFERENTIAL STRAIN ANALYSIS

In differential strain curve analysis (DSCA or DSA), a dry, vertical plug or cubic sample is enclosed in a jacket and hydrostatically compressed, then volumetric contraction is measured. Since the pore pressure is zero, DSA attempts to close the microcracks by externally applying fluid pressure while monitoring the changes in sample dimensions. Linear or diametral contraction is expressed in terms of strain, the change in length per unit length. For an ideal isotropic sample, the pressure-strain relationship, or compressibility, is the same in any direction. However, core samples from reservoirs, whose in-situ stresses are non-hydrostatic may exhibit anisotropic compressibility: maximum contraction occurs along the direction of S_{hmax}, presumably as a result of preferentially oriented microcracks (Strickland and Ren, 1980).

As a laboratory method, time is not a crucial factor as in the on-site tests. Only the homogeneous intervals with reliable compass-scribe or paleomagnetic reference are selected. The transducers used for measuring contraction are resistance-type 3-arm strain gauge-rosettes which are bonded on vertical

cylindrical samples. A whole-core or a 2-inch dia vertical plug has at least 2 gauge-rosettes: 1 set on an end plus 1 set of circumferential gages in the mid-section, Figure 5. A third gauge-rosette may also be added on the other end of the sample. The gauge-rosette data are processed to derive the direction of the principal strain vectors using established routines (e.g. El Rabaa and Meadows, 1986, Strickland and Ren, 1980). Compared to the on-site tests, this version of the DSA technique has the advantage of being more sensitive to the microfractures and less impacted by bedding related structures.

The hydrostatic compression test produces at least 3 pressure-strain curves: one for each arm of the gage-rosette. An example of a pressure-strain curve is shown in Figure 6. In general, the slope is different for each curve, particularly at pressures below 2000 psi. The initial slopes are relatively steep; demonstrating the stress dependency of the void volume. At higher hydrostatic stresses, in the 2000-3000 psi range, the curves gradually become more linear with a flatter slope. The nonlinearity of the DSA curves are interpreted as an effect of the microcracks which are more compressible than the mineral grains (Siegfried and Simmons, 1978). Thus, as the stress-strain plot becomes more linear, it implies that fewer microcracks are being closed and deformation is mostly from grain and pore compaction. If these microcracks are closed above 2000 psi, then they do not enhance effective porosity and permeability at reservoir net confining pressure. At high net confining pressures, the sample is intrinsically isotropic if the pressure-strain curves have identical derivatives.

If the microcracks resulted from stress-relief, then the maximum strain vector is parallel to the azimuth of S_{hmax}. The DSA for Well #1 has maximum strain azimuth ranges of 0-20 degrees, 50-80 degrees, and 140-170 degrees, Figure 7A. The 50-80 degree sector is similar to Well #2's dominant maximum strain azimuths of 80-90 degrees, Figure 7B. There are 21 DSA tests for both wells, and the combined rosette (Figure 7C) has a dominant azimuth of 70-90 degrees. Therefore, the azimuth of maximum contraction is close to Well #2's direction of maximum anelastic expansion but does not confirm Well #1's on-site tests.

VELOCITY ANISOTROPY

In the velocity anisotropy method, ultrasonic compressional (V_p) and vertically-polarized shear (V_s) velocities are measured along nine diametral paths through a core sample, Figure 8A. Microcrack orientation is inferred from the paths of maximum and minimum velocities. Since microcracks impede and deflect the propagation of sonic and ultrasonic energy, the velocity would be fastest (maximum V_p and V_s) along the strike of the microcracks. And as a corollary, the velocity would be slowest (minimum V_p and V_s) along the direction perpendicular to the microcracks' strike. These directions of velocity maxima and minima, if dependent only on stress-relief microcracks, are inferred as the azimuths of in-

situ stresses. For example, the sinusoidal curves of Figure 8B have well defined peaks and valleys for V_p and V_s, whose path of maximum velocity is perpendicular to the path of minimum velocity. However, the V_s-azimuth curves are not as ideal as the V_p sine wave form. For 10 samples from Well #1, the range of V_p is 12569 to 16001 fps (feet/sec), and the range of V_s is 6044 to 9558 fps. The velocity anisotropy index, the ratio of the maximum to minimum velocity, ranges from 1.019 to 1.070.

From V_p anisotropy, the presumed microcrack orientation predicts that S_{hmax} has an azimuth of 50-90 degrees (Figure 9A), while V_s anisotropy leads to an azimuth of 30-70 degrees (Figure 9B). The V_p rosette diagram has less scatter and smaller standard deviation than V_s, implying that V_p anisotropy is better than V_s anisotropy in predicting in-situ stress orientation.

INCIPIENT MACRO-FRACTURES

Incipient macro-fractures are visible natural and coring-induced fractures that can adversely affect whole-core strain tests. The cores have very few natural fractures and these natural fractures are calcite-filled, perpendicular to bedding, and sometimes described as "incipient" fractures. Most of the non-mineralized fractures are coring-induced fractures; these are parallel to the core axis, and in most cases, gradually bend over to intersect the edge of the core. They are also described as scallop, centerline, or petal fractures. The term "coring-induced" is used here as a descriptive term that includes all large, visible "macro-" fractures that resulted from coring; these are non-natural and do not result from anelastic stress-relaxation.

The coring-induced fractures found in both wells appear to have a preferential azimuth. From the rosette diagram of Figure 10, the range of 50-100 degrees contains the majority (58%) of the fractures' strike, and the most dominant azimuth is 50-70 degrees. These large coring-induced fractures are presumed to be parallel to S_{hmax} (Laubach and Monson, 1988). Two of the conditions that may have promoted the development of these large-scale coring-induced fractures are high stress gradients and a rock of high elastic modulus. The stress concentrations at the point of cutting are high and compressive, but the tight sandstone is a high-modulus brittle rock susceptible to tensile failure. Near the face of the bit, the core has been relieved of the vertical stress, S_{vmax}, but the core is still being compressed by S_{hmax} and S_{hmin}. These stress concentrations, combined with pore pressures within a tight and brittle matrix, seem sufficient to induce tensile failure. This is similar to the failure mode of a diametral (Brazilian) tensile strength test (See Jaeger and Cook, 1969 for a description of tensile tests). The maximum stress concentration at the bottom of the well is parallel to S_{hmax}, and estimated to have a magnitude of $1.56 \times S_{hmax}$ (Jaeger and Cook, 1969). This compressive load may be inducing extensional (tensile) stresses parallel to S_{hmin}. The estimated range of the extensional stresses is 400-2000 psi (tensile). The induced

degrees) and shear-velocity anisotropy (30-70 degrees). Thin-section microscopy confirmed the orientation and bimodal-orthogonal distribution of the microfractures, whose major trend predicts an S_{hmax} azimuth of 70-100 degrees.

CONCLUSIONS

- When on-site strain data are ambiguous, multiple methods like differential strain analysis, velocity anisotropy, macro-fracture mapping, and thin-section microscopy can provide consistent predictions of in-situ stress orientation from cores.

- In this tight, well-cemented sand, thin-section microscopy has confirmed the preferential orientation of the microfractures that influence mechanical anisotropy.

LIST OF REFERENCES

Blanton, T.L. and Teufel, L. W., 1983, A field test of the strain recovery method of stress determination in Devonian shale: SPE 12304, Proc. SPE Eastern Regional Mtg., Champion, PA.

El Rabaa, A.W.M. and Meadows, D.L., 1986, Laboratory and field applications of the strain relaxation method: SPE 15072, Proc. 56th SPE California Regional Meeting, Oakland, CA.

Jaeger, J.C. and Cook, N.G.W., 1969, Fundamentals of Rock Mechanics, Chapman and Hall Ltd. and Science Paperbacks.

Lacy, L.L., 1987, Comparison of hydraulic fracture orientation techniques: SPE Formation Evaluation, March.

Laubach, S.E. and Monson E. R., 1988, Coring-induced fractures: Indicators of hydraulic fracture propagation in a naturally fractured reservoir: SPE 18164, Proc. of SPE Annual Technical Conference, Oct. 2-5, Houston, TX.

Owen, L.B., Toronto, T.T, and Peterson, R.E., 1988, Reliability of anelastic strain recovery estimates for stress orientation in the Travis Peak Formation, Harrison County, Texas: SPE 18165, Proc. of SPE Annual Technical Conference, Oct. 2-5, Houston, TX.

Siegfried, R.W. and Simmons, G., 1978, Characterization of oriented cracks with differential strain analysis: J. Geophys. Res., v. 83, pp 1269-1278.

Simmons, G., Siegfried, R.W., and Feves, M., 1974, Differential strain analysis, a new method of examining cracks in rocks: J. Geophys. Res., v. 79, pp 4383-4385.

Strickland, F. G.and Ren, N.K., 1980, Predicting the in-situ stress for deep wells using differential strain curve analysis: SPE/DOE 8594, Proc. SPE/DOE Symp. on Unconventional Gas Recovery, Pittsburg, PA.

Teufel, L.W., 1981, Strain relaxation method for predicting hydraulic fracture azimuth from oriented core: SPE/DOE 9836, Proc. SPE/DOE Low Perm. Symp., Denver, CO.

Teufel, L.W., 1983, Determination of the principal horizontal in situ stress directions from anelastic strain recovery measurements of oriented cores from deep wells: application to the Cotton Valley formation of East Texas: Geomechanics AMD V. 57, pp 55-63.

Teufel, L.W., Hart, C. M., Sattler, A. R., Clark, J. A., 1984, Determination of hydraulic fracture azimuth by geophysical, geological and oriented core methods at the Multiwell Experiment Site, Rifle, Co.: SPE 13226, 9 pp.

Toronto, T.T., and Owen, L.B., 1988, Development of an automated system for field measurement of in-situ stress orientation by the strain recovery method: Poster Paper Proc. 29th U.S. Symposium on Rock Mechanics, Minneapolis, MN.

Table 1

Summary of Results of Core Anisotropy Tests

Test Type	**Predicted S_{hmax} Azimuth** (degrees)
On-site anelastic strain, #1	00- 30 (Well #1), anomaly
On-site anelastic strain, #2	90-120 (Well #2)
Laboratory DSA	70- 90
Compressional Velocity	50- 90
Shear Velocity	30- 70
Coring-induced fractures	50- 70
Thin-section microscopy	70-100

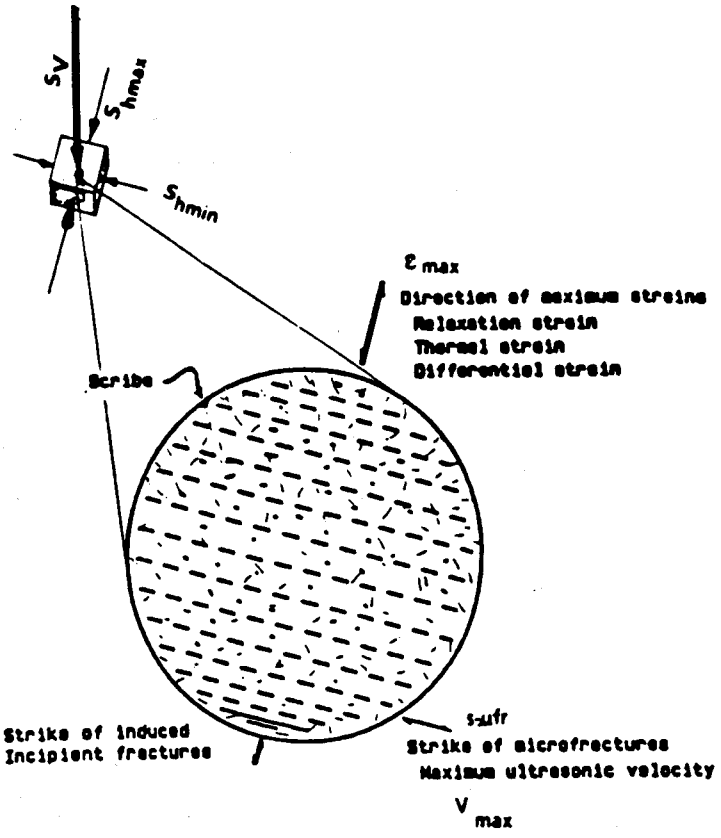

Figure 1. Idealized microcrack distribution and directions of mechanical anisotropy.

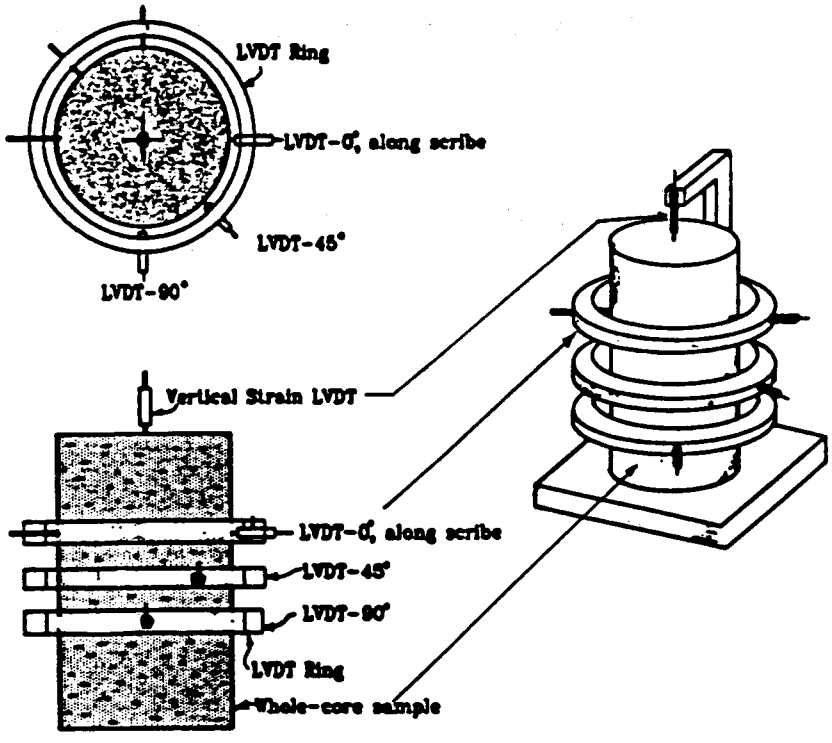

Figure 2. Instrumentation of a core sample for anelastic strain tests using linear variable displacement transducers (LVDT).

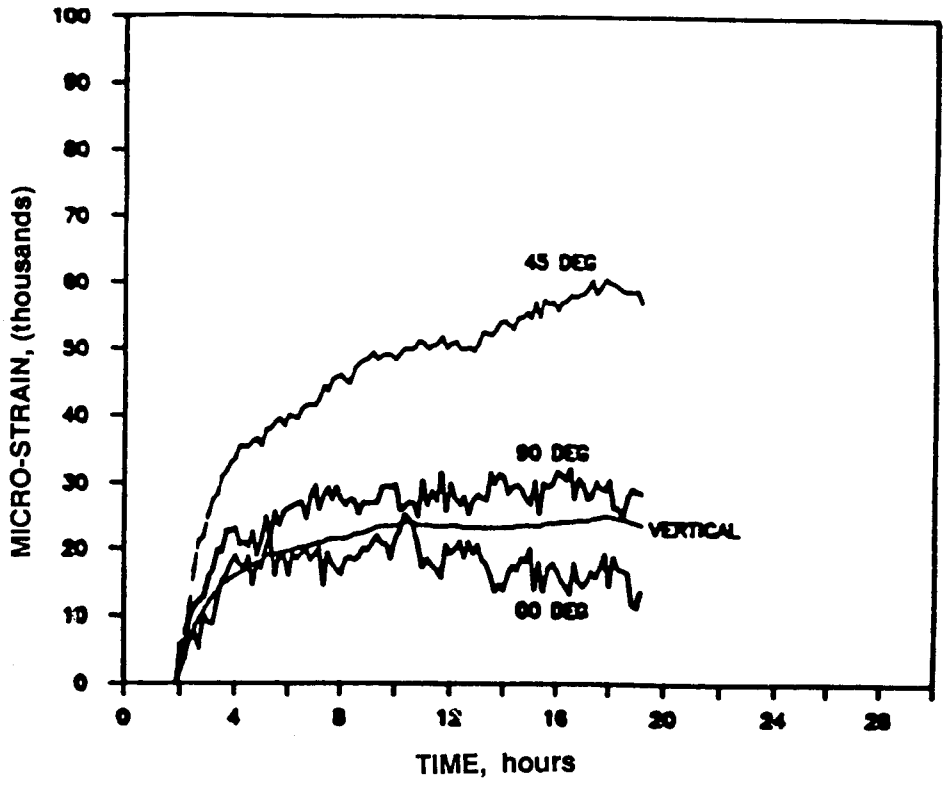

Figure 3. Example of strain relaxation curve.

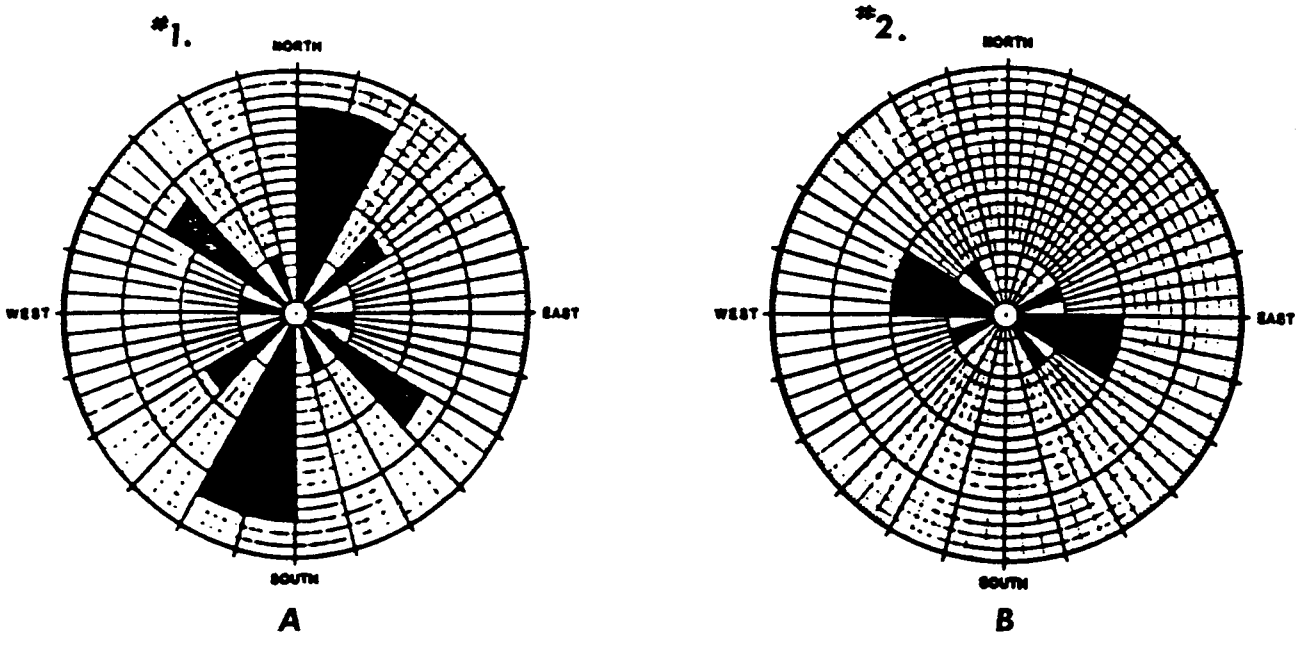

Figure 4. Rosette diagrams of maximum on-site strains,
A. Well #1, B. Well #2

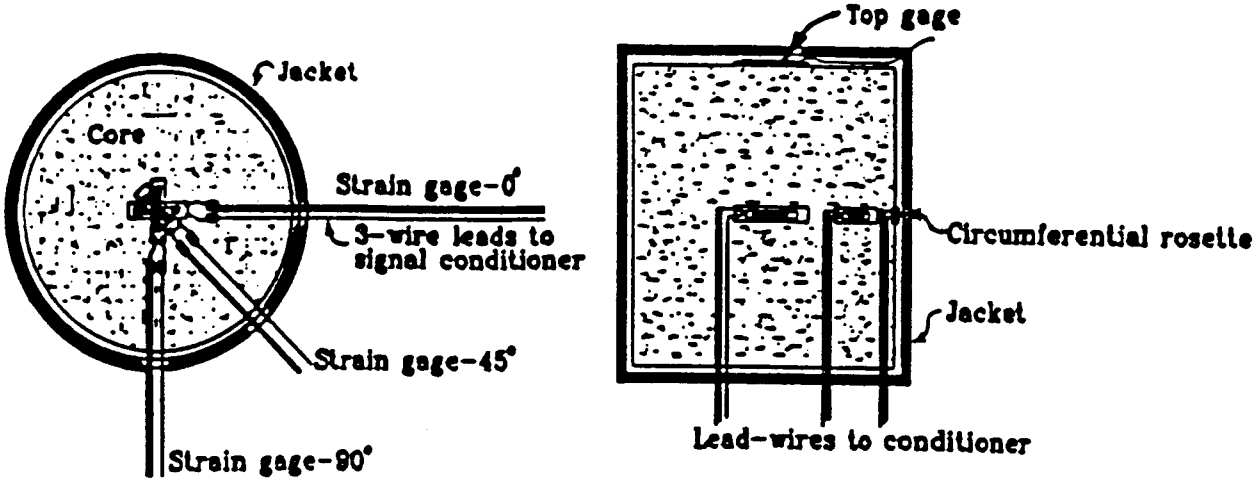

Top View Side View

Figure 5. Vertical core sample instrumented for laboratory differential strain analysis (DSA).

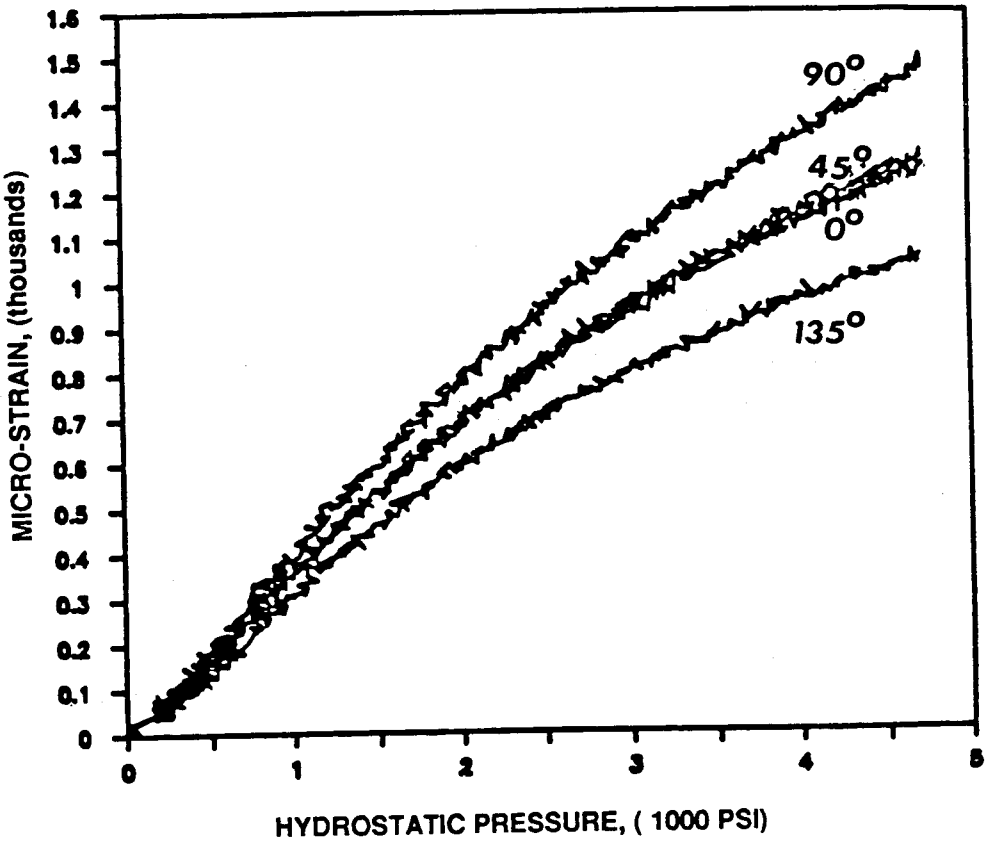

Figure 6. A set of stress-strain curves from laboratory DSA.

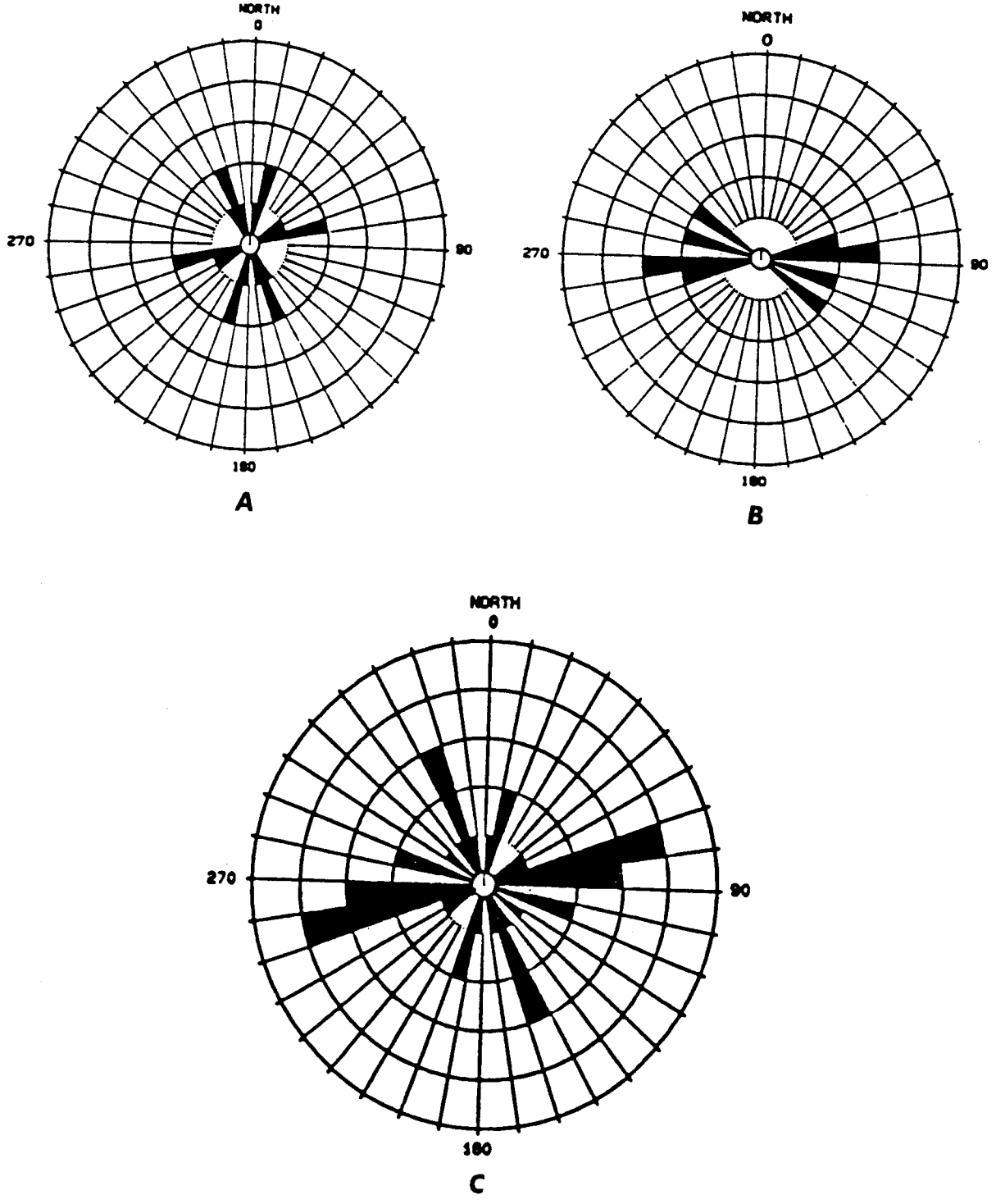

Figure 7. Rosette of maximum differential strains
A. Well #1, B. Well #2, C. Combined Well #1 and #2.

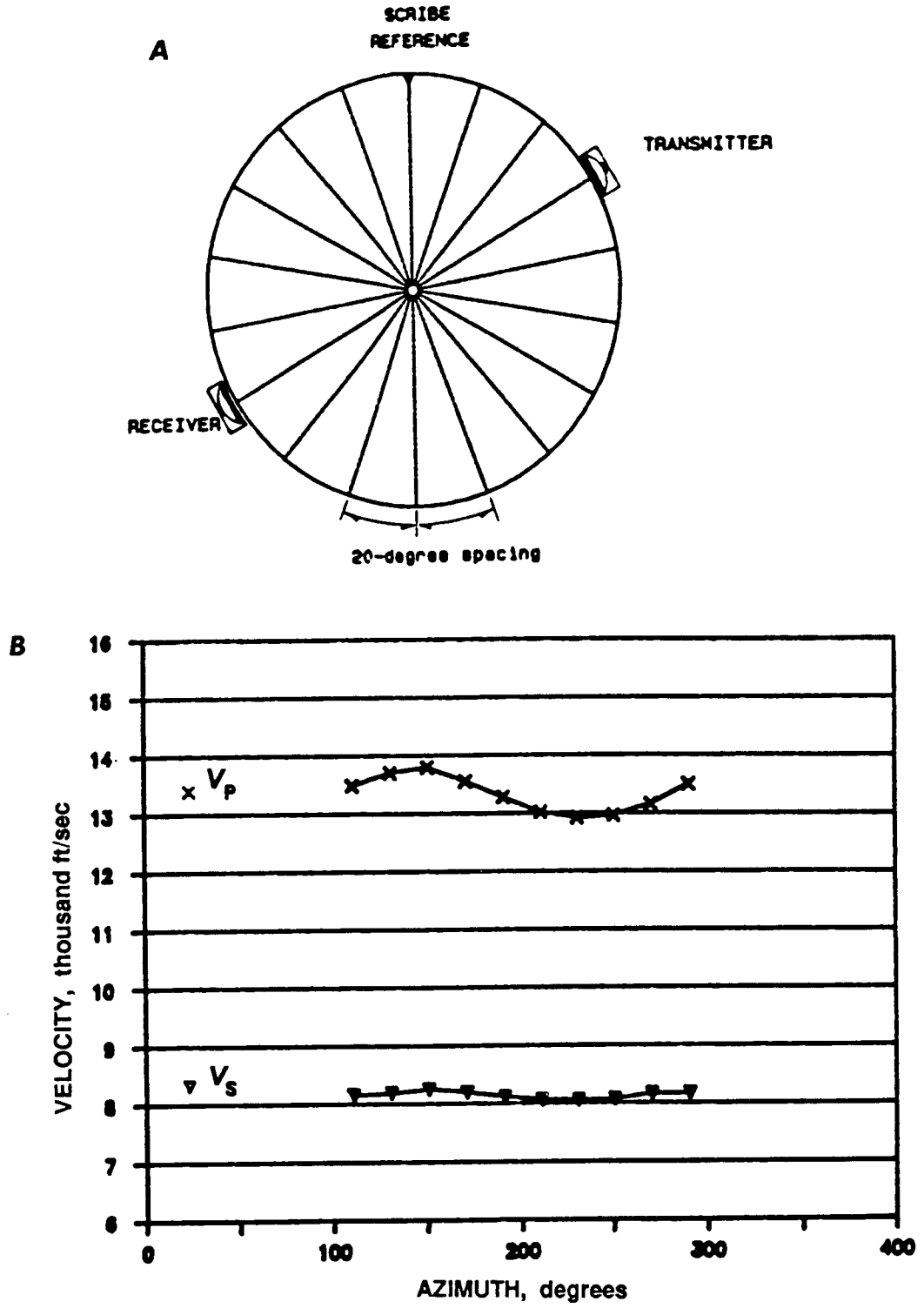

Figure 8. A. Velocity anisotropy transducer setup.
B. Ideal sinusoidal shape of velocity-azimuth curve.

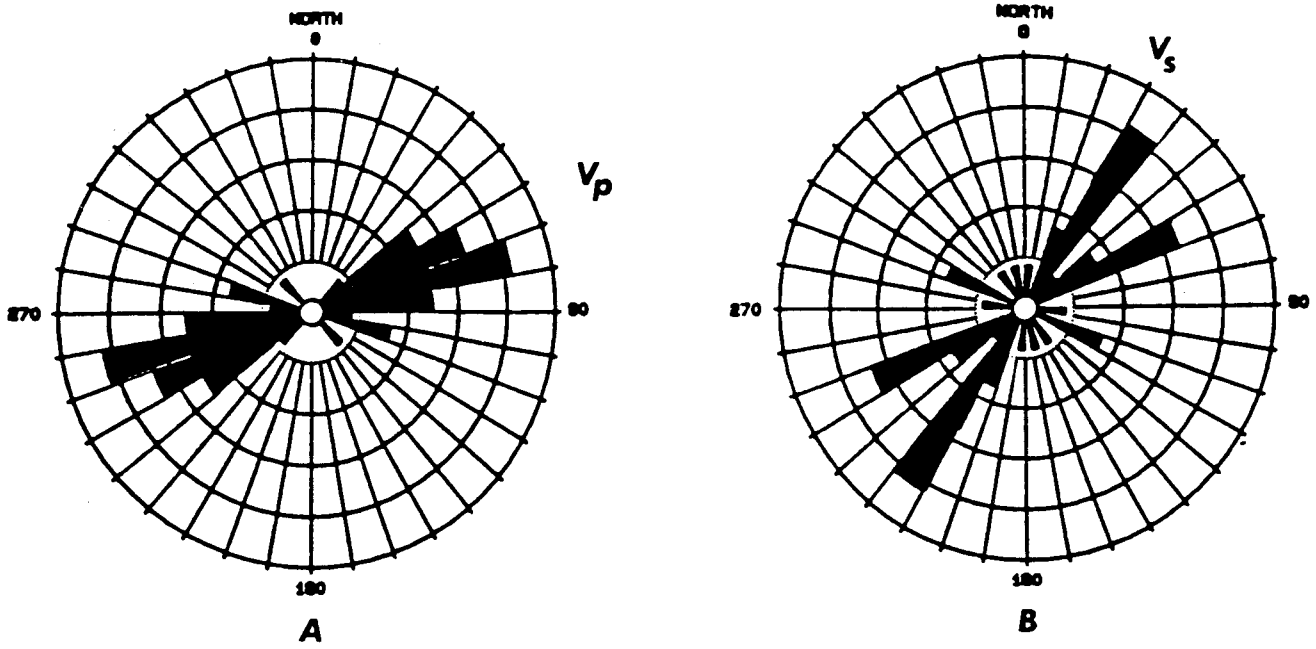

Figure 9. Velocity anisotropy rosette diagrams:
A. V_p anisotropy, B. V_s anisotropy.

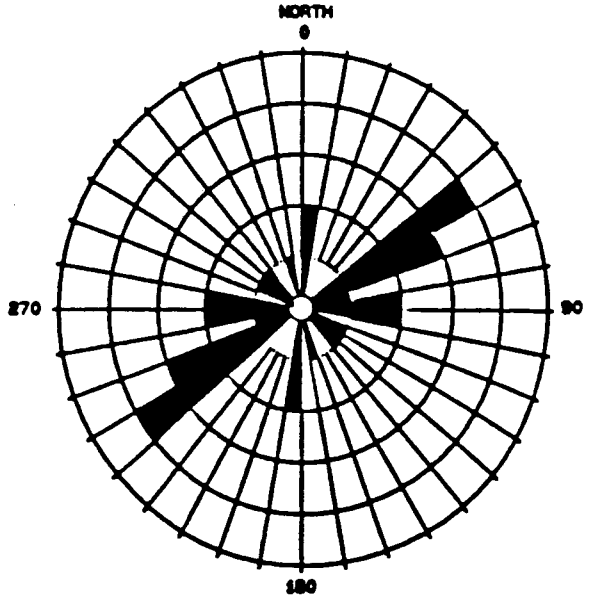

Figure 10. Rosette diagram of strikes of incipient fractures.

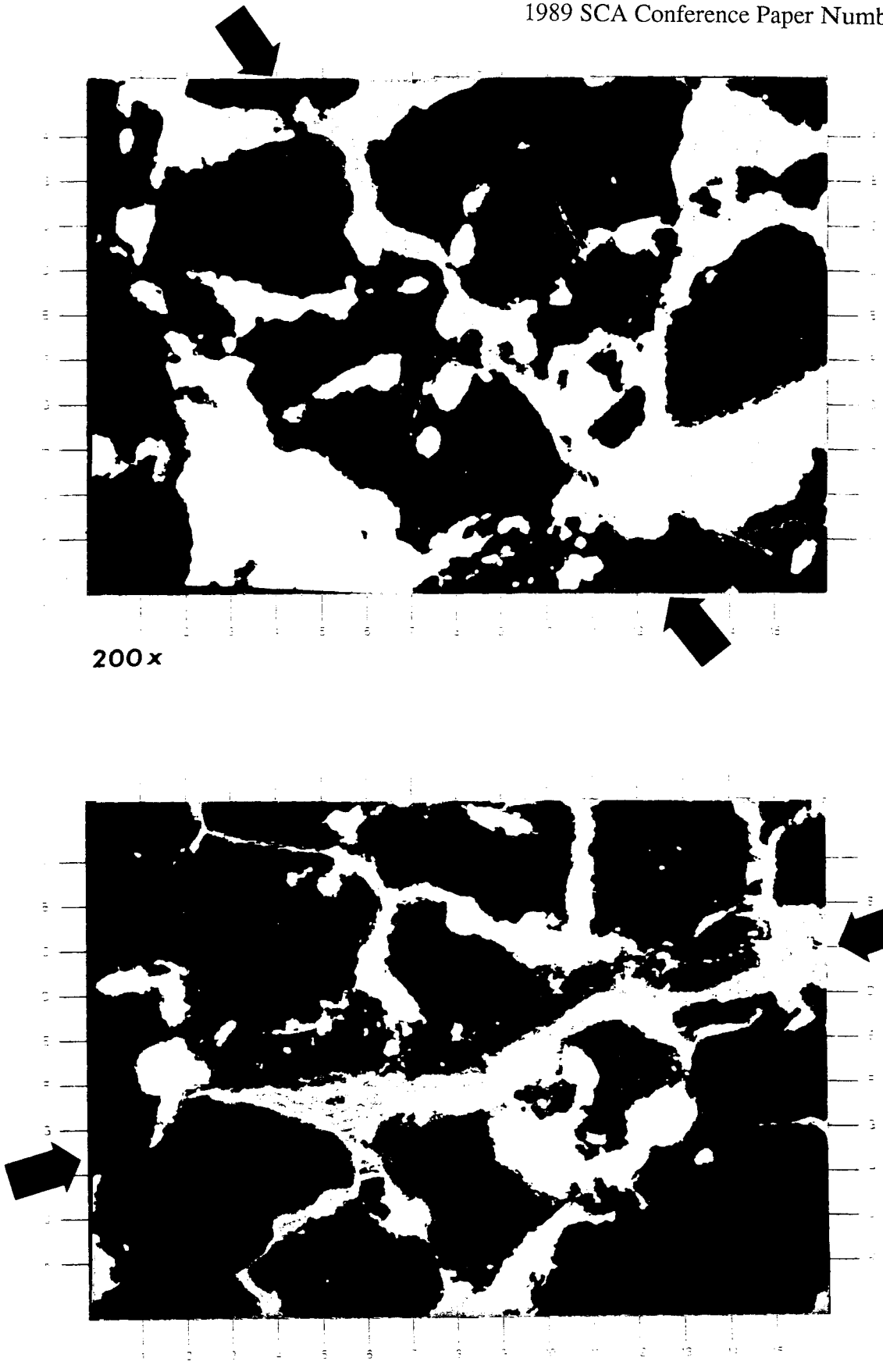

Figure 11. Examples of microfractures observed with fluorescent thin-section microscopy.

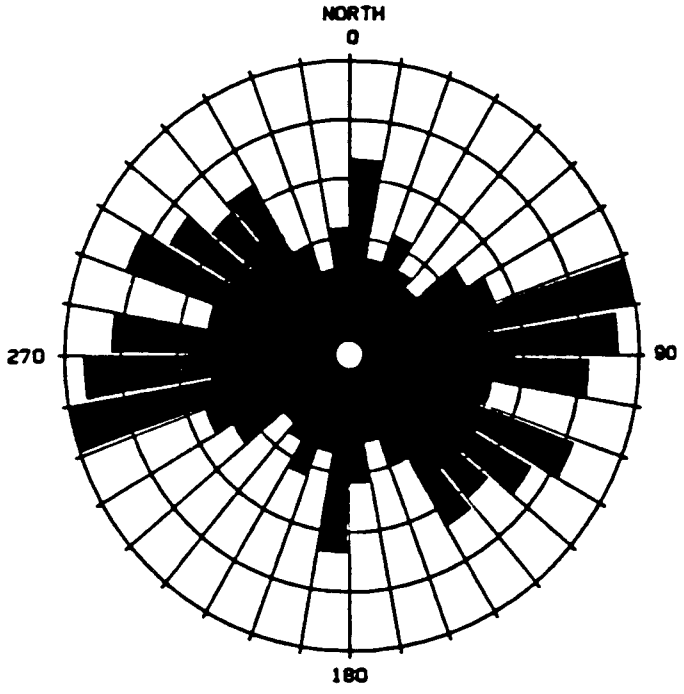

Figure 12. Rosette diagram of inferred azimuth of S_{hmax} from thin-section microfracture mapping.

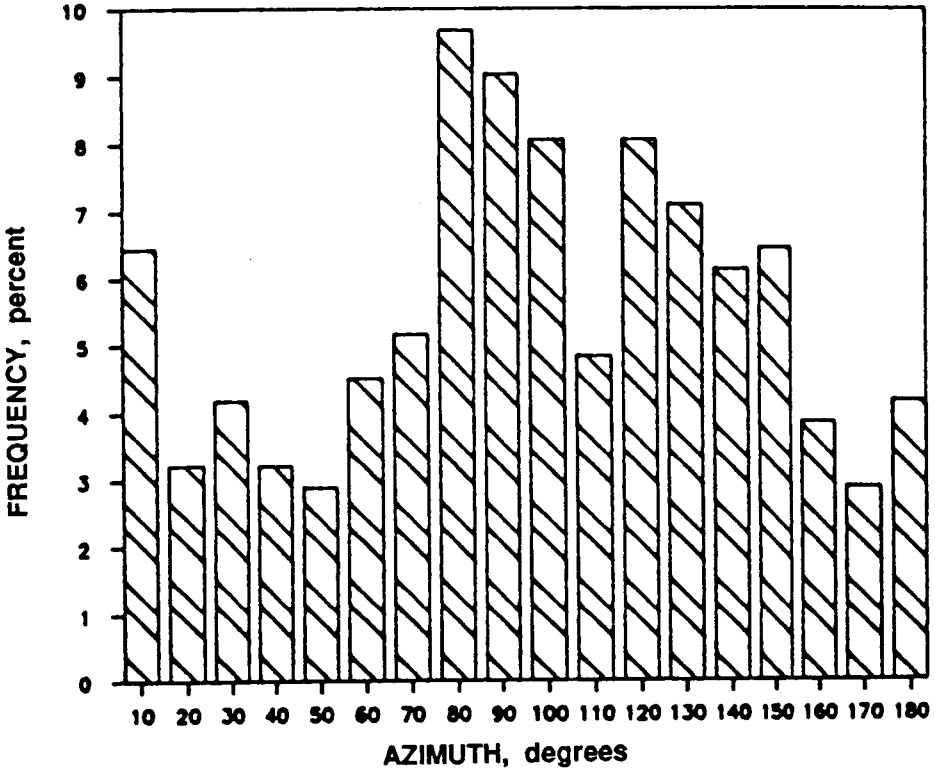

Figure 13. Frequency histogram of inferred azimuth of S_{hmax} from thin-section microfractures.